Magnetic Resonance Imaging 59 (2019) 10–16

Contents lists available at ScienceDirect

Magnetic Resonance Imaging

journal homepage: www.elsevier.com/locate/mri

Original contribution

Age-related changes in eye morphology and aqueous humor dynamics in DBA/2J mice using contrast-enhanced ocular MRI

Darragh E. Crosbie[a,1], James Keaney[a,b,1], Lawrence C.S. Tam[a], W. Daniel Stamer[c], Matthew Campbell[a,*], Peter Humphries[a,*]

[a] Ocular Genetics, Unit, Smurfit Institute of Genetics, Trinity College Dublin, Lincoln Place Gate, Dublin 2, Ireland
[b] Ross University School of Veterinary Medicine, P. O. Box 334, Basseterre, St. Kitts, Saint Kitts and Nevis
[c] Departments of Ophthalmology and Biomedical Engineering, Duke University, Durham, NC, USA

ARTICLE INFO

Keywords:
Glaucoma
Aqueous
Vitreous
Trabecular meshwork
Contrast enhanced MRI
Outflow

ABSTRACT

Purpose: Here, we are testing the hypothesis that dynamic contrast enhanced MRI (DCE-MRI) is a useful approach for non-invasively evaluating age-related changes in aqueous humor outflow and its contribution to elevated intraocular pressure in the DBA/2J model of pigmentary glaucoma.

Methods: A rodent-specific 7 T MRI was used to assess eye anatomy (anterior chamber (AC) and vitreous body (VB) morphology, eye size, lens size) and aqueous humor dynamics (via intravenous administration of Gd-DTPA and Gd-BOPTA contrast agents) in C57BL/6 and DBA/2J mice at 3 and 9 months of age.

Results: Gd-MRI was used to demonstrate an anterior solute pathway into the mouse AC. Topical latanoprost treatment in C57BL/6J mice reduced Gd-BOPTA accumulation in the AC. Age-related increases in AC area, AC depth and eye size were observed in DBA/2J mice compared to C57BL/6J mice. The rate of Gd-DTPA accumulation and peak Gd-DTPA intensity was lowest in 9-month old DBA/2J mice compared to 3-month old DBA/2J mice and C57BL/6J mice at both ages. Leakage of Gd-DTPA posteriorly into the VB was also observed in 9-month old DBA/2J mice.

Conclusions: These studies support the idea that age-related changes in aqueous humor outflow contribute to elevated intraocular pressure (IOP) in the DBA/2J model of pigmentary glaucoma. Gd-MRI is a valuable tool for better understanding of mechanisms and dynamics of aqueous humor circulation in normal and glaucomatous mouse eyes or following topical administration of medicines to reduce IOP.

1. Introduction

Pigment dispersion syndrome is characterized by shedding and dispersion of iris pigment throughout the anterior (AC) and posterior chambers (PC) of the eye [1]. It is often associated with elevated intraocular pressure (IOP) that can lead to damage of the optic nerve and pigmentary glaucoma, a form of secondary open-angle glaucoma that tends to affect younger people [2]. The DBA/2J mouse strain recapitulates many facets of human pigmentary glaucoma such as pigment dispersion, iris atrophy, iris transillumination and elevated IOP [3,4], though unlike the human condition, angle closure is a feature of this strain due to the development of anterior synechias (attachment of the anterior iris to the trabecular meshwork) and dysgenesis of outflow structures [3]. Elevated IOP presents at 2–6 months in DBA/2J mice, reaching a peak at 9–11 months; resulting in retinal ganglion cell loss and optic nerve cupping [5–8].

Regulation of aqueous humor secretion and drainage are integral to maintaining physiological IOP and data show that age-related IOP increases in glaucomatous eyes stem from disruption of the conventional outflow pathway [9]. In the case of the DBA/2J mouse model, mutations in the *Tyrp1* and *Gpnmb* genes induce iris atrophy and pigment dispersion [10,11], processes which are thought to affect aqueous humor outflow at the trabecular meshwork. However, the dynamics of aqueous humor secretion and drainage in normal and glaucomatous mouse eyes are still unresolved and little is known about aqueous humor flow changes in pigmentary glaucoma.

Magnetic resonance imaging (MRI) using contrast agents like gadolinium diethylene-triamine penta-acetic acid (Gd-DTPA) or manganese (Mn^{2+}) has been used to assess ocular anatomy [12–14], retinal blood flow [15], blood-retina barrier permeability [16] and aqueous

* Corresponding author.
E-mail addresses: matthew.campbell@tcd.ie (M. Campbell), Pete.Humphries@tcd.ie (P. Humphries).
[1] Joint first authors.

https://doi.org/10.1016/j.mri.2019.01.016
Received 1 October 2018; Received in revised form 15 January 2019; Accepted 16 January 2019

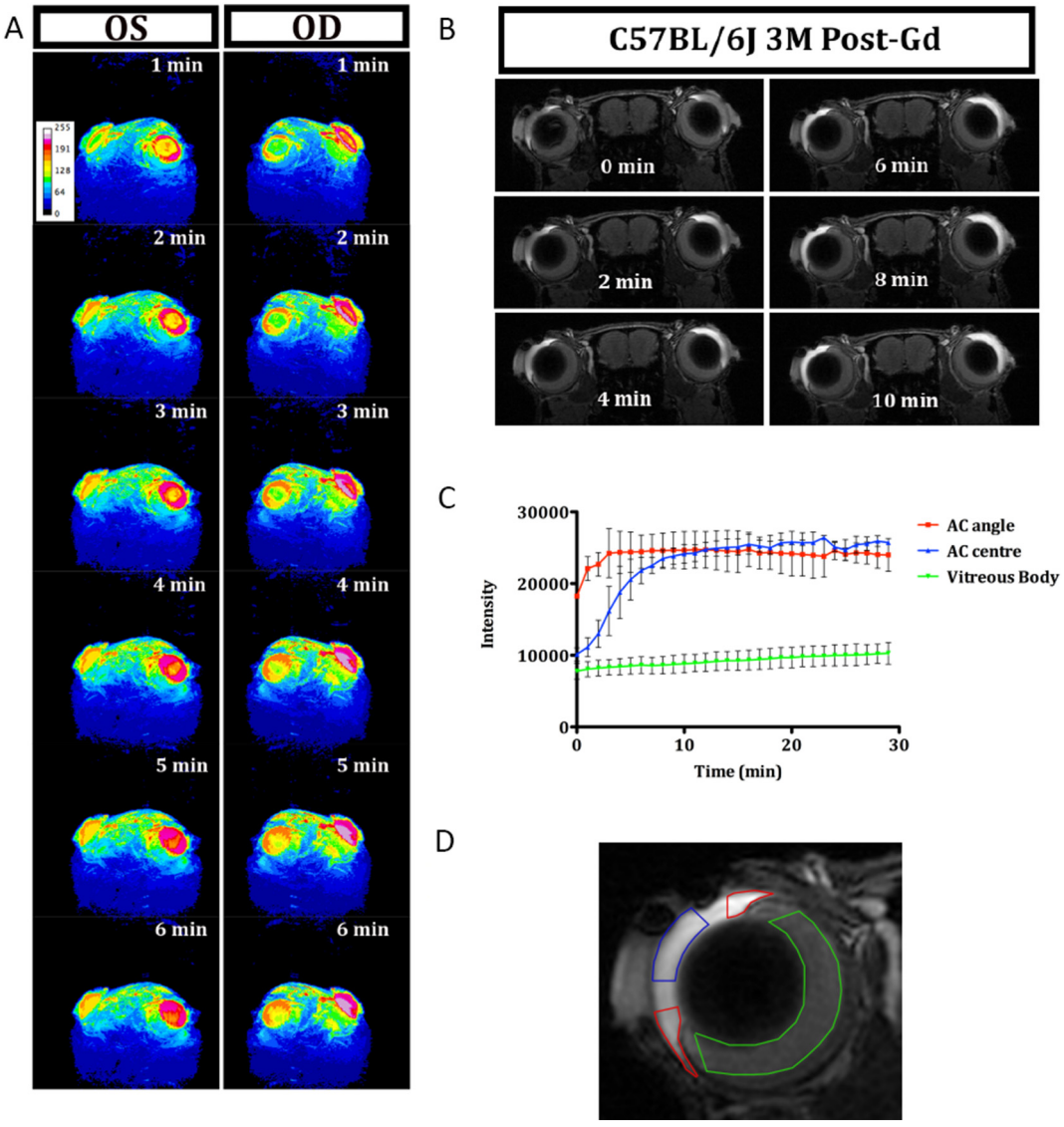

Fig. 1. Entry of Gd-DTPA into the AC via the anterior protein pathway.
A 3-D rendered image of Gd-DTPA entry into the AC over time, representing the OS and OD eyes of a single animal, image is pseudo-colored to represent pixel intensity with attached intensity scale in image OS = 1 min. B Representative image of T_1 MRI scan of a 3 M C57BL/6J mouse demonstrating Gd-DTPA entry over time. C Pixel intensity in the AC angle, AC centre and VB over time after Gd-DTPA injection. D Representation of areas used for pixel intensity measurement. Red = AC angle; blue = AC centre; green = vitreous body. In all figures Time = time after Gd-DTPA injection with injection at 0 min. (For interpretation of the references to color in this figure legend, the reader is referred to the web version of this article.)

humor flow [17,18] in rodents, monkeys and humans, among other species. Gd-DTPA and Gd-BOPTA are water-soluble passive tracers (938 Da and 600 Da, respectively) that under homeostatic conditions can cross the blood-aqueous barrier following systemic administration but have not been reported to cross the blood-retinal under normal conditions [17–19]. Gadolinium tracer has previously been used to demonstrate an anterior diffusional pathway for solutes into the aqueous humor [18–22]. Clearance of aqueous humor and solutes from the AC occurs primarily via the conventional outflow pathway consisting of the trabecular meshwork and Schlemm's canal (SC) and secondarily via the unconventional pathway between the ciliary muscle fibers (often referred to as the uveoscleral route) [9].

In the present study, the diffusion of gadolinium tracer into the anterior chamber was characterized in mice. Gd-BOPTA enhanced MRI was used to assess total rates of aqueous humor flow and ocular permeability in the mouse eye following topical administration of latanoprost, a prostaglandin $F_{2\alpha}$-receptor analogue that alters aqueous humor outflow. Though the first-line treatment for ocular hypertension, latanoprost's mechanism of action is as yet to be fully elucidated. Traditionally its effects have been ascribed to an increase in drainage through the ciliary muscle in humans, however it has been shown to also increase outflow through the trabecular meshwork, FP receptor activation leading to matrix-metalloproteinase (MMP) activation within the TM [23,24].

Having established the ability of Gd-enhanced MRI to detect flow changes through the AC, this was followed by assessment of aqueous humor dynamics at different ages in the DBA/2J mouse model of pigmentary glaucoma with age-matched C57BL/6J mice as controls using Gd-DTPA. These data indicate that blood-aqueous barrier breakdown accompanies age-related changes in AH dynamics in the DBA/2J mouse.

2. Materials and methods

2.1. Animals

Wild-type C57BL/6J mice were sourced from Jackson Laboratories and bred on-site in the Smurfit Institute of Genetics in Trinity College Dublin (TCD). DBA/2J mice were obtained from Harlan, UK. Animals were housed under a 12-hour light–dark cycle and were provided unrestricted access to food and water. For latanoprost administration, each mouse received three doses of 50 mg/ml latanoprost eye-drops (Monopost Unidose, Thea Laboratories) at 24 h, 12 h and 3 h prior to MRI imaging. The contralateral eye was dosed with saline eye-drops simultaneously as a control. All procedures involving experimental animals were performed in accordance with the ARVO Statement for Use of Animals in Ophthalmic and Vision Research and were approved by the Institutional Ethics Committee in University of Dublin, Trinity College, under the HPRA project authorization AE19136/P017.

2.2. Contrast-enhanced magnetic resonance imaging (MRI) and data analysis

Aqueous humor flow was assessed using a dedicated small rodent 7 T MRI system (Bruker BioSpec) at TCD. Tetracaine hydrochloride (1% w/v, Bausch and Lomb) was applied to both eyes to minimize eye movement and visidic eye gel (0.2% w/w, Bausch and Lomb) was used to prevent corneal dryness. Mice were anaesthetized with 5% isoflurane and placed on an MRI-compatible support cradle. This cradle has an in-built system for maintaining the animal's body temperature at 37 °C and a probe underneath the animal allows it to be physiologically monitored (electrocardiogram, respiration and temperature). To ensure accurate positioning of the animal, an initial rapid pilot image was recorded and used to ensure correct geometry for all subsequent scans. Blood-aqueous barrier integrity and aqueous humor flow were then visualized in high-resolution T1-weighted MR images before and after intravenous (tail vein) administration of 200 μl of 0.17 mmol/ml Gd-DTPA (Gadolinium diethylene-triamine penta-acetic acid, Magnevist, 0.5 mmol/ml stock solution, Bayer) or Gd-BOPTA (Gadobenate dimeglumine, MultiHance, 529 mg/ml stock solution, Bracco), which was monitored over a period of 60 mins post-injection. MR images specifications were as follows: resolution: $63 \times 63\,\mu m^2$; field of view: $16 \times 16\,mm^2$; in-plane resolution: 256 × 256 pixels; slice thickness: 0.25 mm; repetition time/echo time: 409/7 ms; flip angle: 30°; number of averages: 1; acquisition time: 1 min, 10 s; repetitions: pre-scan — 4, post-scan — 60. MR image analysis was performed using *ImageJ* and *MIPAV* software and all data was analyzed blind to treatment. For change in intensity analysis the baseline was taken from Time (0 min) after Gd-DTPA injection and rate of increase was calculated from a linear fit over the initial 10 min period.

2.2.1. Ocular anatomy

Fig. 1 shows the major regions of interest for morphological analyses. The following structures and measurements were recorded using the pre-Gd-DTPA MRI scans and *ImageJ* software — AC area, AC signal intensity, AC depth, VB area, VB signal intensity, VB depth, lens size and eye size.

2.2.2. T1-weighted Gd-DTPA enhancement

AC signal intensity post-Gd-DTPA or Gd-BOPTA administration was calculated and 3-D images were constructed with *ImageJ* software.

2.3. Statistics

For each data set, the mean (μ), standard deviation (s.d.) and standard error of the mean (s.e.m.) were calculated. A two-tailed unpaired Student's *t*-test was used to evaluate the significance of differences between each data set. Differences were considered statistically significant when P values were ≤ 0.05. For multiple comparisons across groups, one-way ANOVA followed by Bonferroni's post hoc tests was used with $P \leq 0.05$ representing significance.

3. Results

Firstly, the dynamics of Gd-DTPA diffusion into the AH was examined. 3 M C57BL/6J mice were intravenously injected with Gd-DTPA (Time = 0 min) and immediately after these animals were examined with MRI, taking a scan every minute. 3-D rendered images of the T_1 scan were pseudocolored based on pixel intensity to more easily demonstrate differences in T_1 signal. In both these images the signal enhancement of the AH by Gd-DTPA was first seen as a ring at the iridocorneal angle at $T = 1$ min. Over the course of the next 6 min the contrast agent was seen to diffuse throughout the AC reaching a homogenous state (Fig. 1A). Similarly, in the 2-D images signal enhancement begins at the iridocorneal angle ($T = 0$ min) and diffuses throughout the AC ($T = 10$ min) (Fig. 1B). The mean signal intensity of the AC angle, AC centre and VB were measured and compared over time. The VB displays no evidence of Gd-DTPA entry with only a slight increase in signal over 30 mins, which is consistent with MRI scan variation (n = 4). The signal at the AC angle was immediately higher at $T = 0$ min and reached a max at $T = 3$ min before plateauing (n = 2). In the AC centre the signal was similar to the VB at $T = 0$ min before increasing and reaching a similar max as seen in the AC angle at $T = 20$, from where it plateaued for the remaining scan time (n = 2) (Fig. 1C). The ocular areas where signal intensity was measured are shown in (Fig. 1D). These results demonstrate that Gd-DTPA enters the mouse AH at the iridocorneal angle and not at the ciliary body (CB).

In order to test the applicability of Gd-enhanced MRI to detect aqueous humor flow changes in the mouse eye, C57BL/6 mice were topically administered latanoprost (or saline in the contralateral eye) at 24 h, 12 h and 3 h prior to MRI scanning. Intravenous administration of Gd-BOPTA followed by T_1-weighted MRI revealed that the signal-enhancement in the AC of the latanoprost-treated eyes was significantly lower than that of controls (rate of increase; saline: 1.6%/min, latanoprost: 0.3%/min, $^*P \leq 0.05$) (Fig. 2A). Peak percentage intensity in Gd-BOPTA signal enhancement was also lower in latanoprost-treated eyes compared to contralateral saline treatment (peak intensity; saline: 31.2%, latanoprost: 17.2%, $P = 0.26$) (Fig. 2B). During the initial 20 min the latanoprost treated eyes had a more rapid increase in signal intensity and reached a higher peak than the saline treated eyes, both then reach a plateau before gradually declining over the remaining scan period (Fig. 2C).

Gd-enhanced MRI was then applied to the DBA/2J model of pigmentary glaucoma. Prior to Gd-DTPA administration, pre-contrast images were used to assess various aspects of eye morphology in 3, 6 and 9 month-old DBA/2J mice and compared to age-matched C57BL/6J mice. Representative MR images in Fig. 3A show clear age-related increases in AC area, AC depth and eye size in DBA/2J mice as compared to age-matched C57BL/6J mice. IOP measurements in DBA/2J mice compared to WT control mice showed increased IOP at 6 and 9 months in DBA/DJ mice compared to the same animals at 3 months of age ($^{**}P \leq 0.01$).

Quantification of AC area and AC depth showed increases that were significant at 6 months of age in DBA/2J mice when compared to age-matched C57BL/6J mice (AC area: 12.9% increase, $^*P \leq 0.05$; AC depth: 24.3% increase, $^{**}P \leq 0.01$) and which were even more pronounced at 9 months of age when compared to age-matched C57BL/6J mice (AC area: 17.8% increase, $^{***}P \leq 0.001$; AC depth: 49.6% increase, $^{***}P \leq 0.001$) (Fig. 3C). Signal intensity pre-contrast enhancement of the AC and overall eye size was significantly increased in DBA/2J at 9 months of age in comparison to age-matched C57BL/6J controls (AC signal intensity: 44.1% increase, $^{***}P \leq 0.001$; eye size: 9.0% increase, $^{***}P \leq 0.001$). Measurements of other ocular components – vitreous body (VB) area, VB signal intensity, VB depth and lens size –

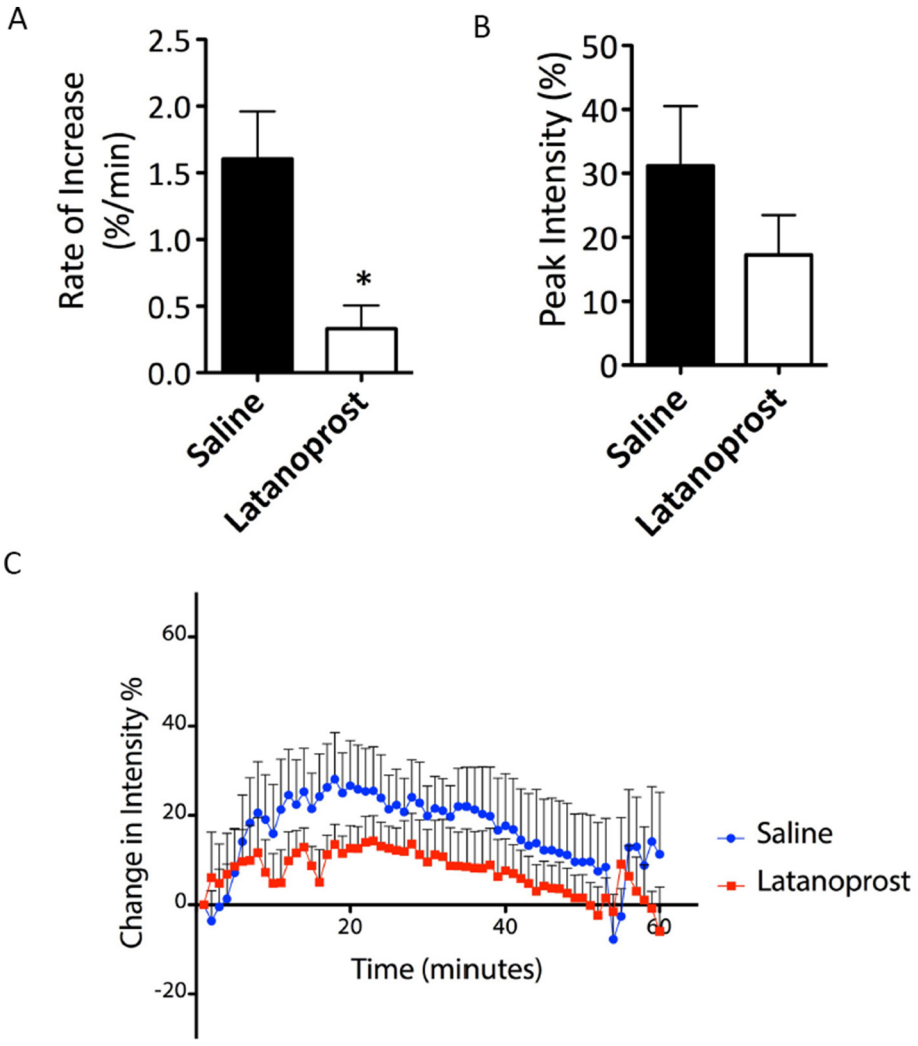

Fig. 2. Effects of latanoprost on aqueous humor flow dynamics in C57BL/6 mice.
A. The rate of Gd-DTPA increase (%/min) in the AC during the 10 min after Gd-DTPA injection was compared between latanoprost-treated eyes and contralateral saline-treated eyes. Gd-DTPA enhancement of the AC was significantly decreased in latanoprost-treated eyes. (Unpaired Student's *t*-test, 95% confidence interval, n = 4 animals, $^{*}P = 0.0184$. Data are means ± s.e.m). B. Peak Gd-DTPA intensity in the AC was compared between latanoprost- and saline-treated eyes. C. The average percentage change in intensity (relative to time (0 min) after Gd injection) over an hour in saline and latanoprost treated C57 eyes (n = 4 animals, data points are means ± s.e.m).

showed no significant differences with age or between DBA/2J and C57BL/6J strains (Fig. 3C).

Following Gd-DTPA administration, T1-weighted MRI showed a reduced signal enhancement of the AC in 9 month-old DBA/2J mice compared to age-matched C57BL/6J animals: sample images are shown in Fig. 4A. Analysis of the percentage change in signal intensity in the first 10 min post-Gd-DTPA injection showed that signal enhancement was lowest in 9 month-old DBA/2J mice (Fig. 4B). The extent of AC signal enhancement in 3 month-old DBA/2J animals was comparable to 3 month- and 9 month-old C57BL/6J mice. Furthermore, the rate of Gd-DTPA accumulation in the AC over the initial 10 min was significantly lower in the DBA/2J 9 month eyes relative to age matched controls (Rate of increase; C57 9 m: 14.0%/min, DBA 9 m: 3.7%/min, $^{**}P \leq 0.01$) (Fig. 4C), no significant difference was seen between the 3 month DBA/2J and age matched C57 mice or between 3 month and 9 month DBA/2J mice. Similarly the peak percentage intensity in Gd-DTPA signal enhancement (Fig. 4D) was lowest in 9 month-old DBA/2J mice, although statistical significance was not reached.

T1-weighted imaging following Gd-DTPA administration also revealed significant leakage of Gd-DTPA into the VB of 9 month-old DBA/2J mice but not age-matched C57BL/6J animals (Fig. 5A). At early stages post-Gd-DTPA injection, the contrast agent appeared to be emanating from the ciliary body and diffusing toward the posterior VB, indicating a breakdown in aqueous-vitreous barrier integrity in the ciliary bodies. Analysis of percentage change in Gd-DTPA intensity using a region of interest in the anterior VB showed prolonged leakage of Gd-DTPA in the VB for as long as 60 mins post-Gd-DTPA injection (Fig. 5B).

4. Discussion

In this study, dynamic contrast-enhanced MRI was used to investigate aqueous humor dynamics and blood-aqueous barrier permeability in the DBA/2J mouse model of pigmentary glaucoma and to identify age-related changes in these phenotypes. Here, we sought to verify the use of Gd-DTPA-enhanced MRI to quantify aqueous humor tracer accumulation in the AC of normal and glaucomatous mouse eyes. Gd-DTPA was found to enter the AC via the anterior iris route, as has been demonstrated in both rabbit and human [18,25]. Additionally, AH dynamics in mouse appear to be similar to human and we show that the anterior solute pathway also exists in mouse, confirming its utility as a good model system for glaucoma studies.

The AC anterior protein pathway is not intrinsically linked to AH production with AH protein concentration levels highest at times when AH secretion is low, such as after treatment with the cholinergic drug pilocarpine [26,27]. Therefore, increasing AH drainage should increase gadolinium-tracer drainage and reduce signal enhancement in these eyes. To investigate this, eyes were treated with the IOP-lowering medication latanoprost. Gd-BOPTA was used as the contrast agent in this study as it entered via the same pathway as the Gd-DTPA and to demonstrate this techniques utility with various MRI contrast agents. Topical application of latanoprost in C57BL/6 mice resulted in reduced

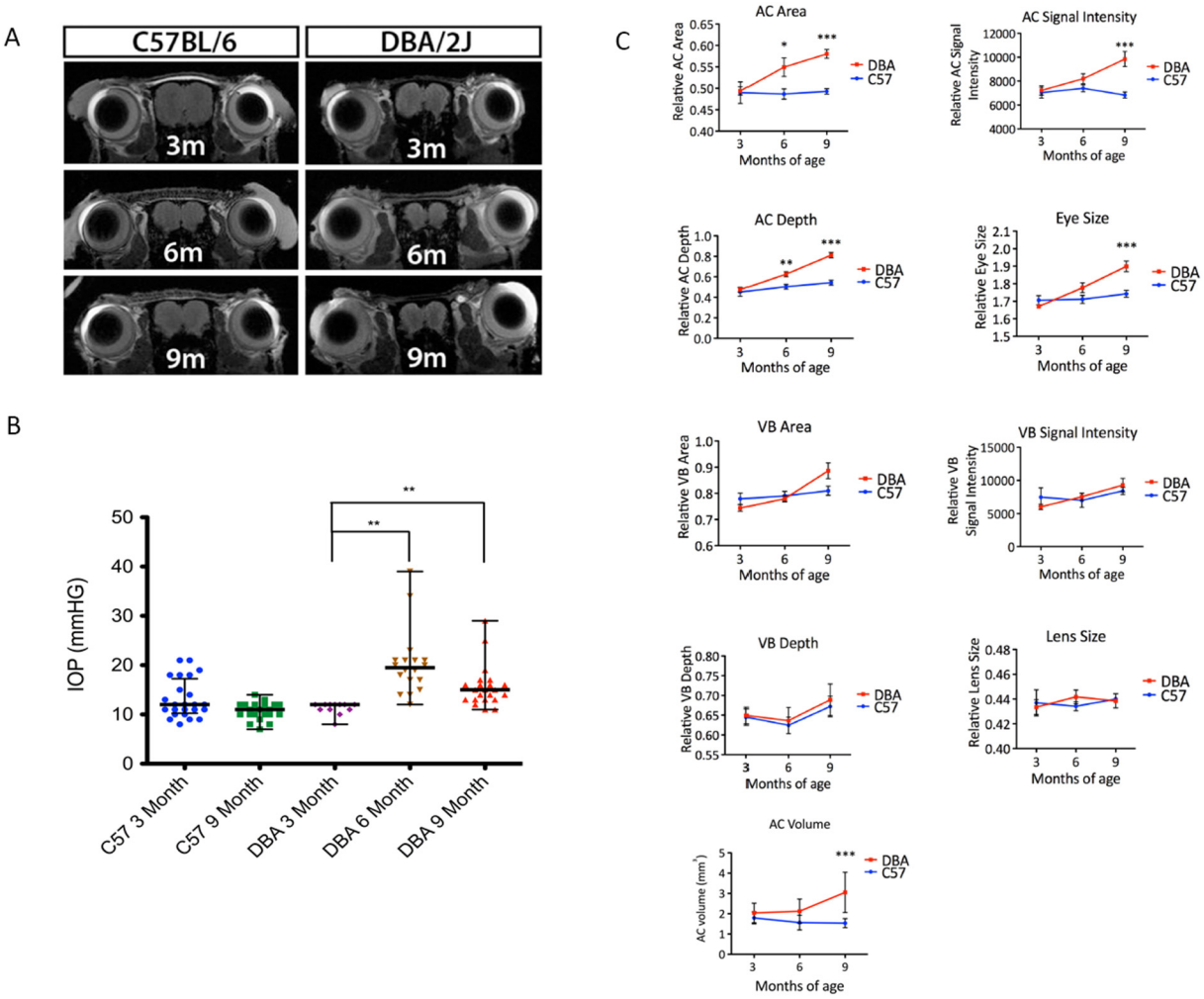

Fig. 3. Morphological analysis of eye anatomy in C57BL/6 and DBA/2J mice using T1-weighted MRI.
A. Representative MR images of eye morphology in C57BL/6 and DBA/2J mice at 3, 6 and 9 months of age. B) Intraocular pressure measurements in DBA/DJ mice at 3, 6 and 9 months compared to wild-type mice (**$P \leq 0.01$). C. Quantification of area, depth and signal intensity of AC and VB, along with lens and eye size in C57BL/6 and DBA/2J mice at various ages. Age-related increases in AC area, AC signal intensity, AC depth and eye size were observed in DBA/2J mice in addition to aqueous volume. (One-way ANOVA followed by Bonferroni's post hoc test for multiple comparisons, 95% confidence interval, $n = 3$–5 separate animals per age and strain, *$P \leq 0.05$, **$P \leq 0.01$, ***$P \leq 0.001$. Data are means ± s.e.m.).

rates of Gd-BOPTA signal enhancement and peak Gd-BOPTA intensity in the AC, indicative of a change of Gd-accumulation in the ACs of latanoprost treated eyes. This clearance of gadolinium from the AC in latanoprost-treated eyes in the first 10 min after Gd-BOPTA injection also demonstrates the ability of contrast-enhanced MRI to identify and track dynamic changes in aqueous humor flow within the AC. Interestingly, latanoprost has a mechanism of action that affects both the conventional and non-conventional outflow pathways. Latanoprost can induce MMP activation, and therefore have a cytoskeletal effect on trabecular meshwork (TM) cells. It can also induce calcium activated potassium currents, which relaxes the TM cells and increases outflow. This has been observed in human subjects manifested by IOP changes with tonography [28–31].

Iris atrophy and pigment dispersion have previously been associated with elevated IOP and degeneration of retinal ganglion cells in the DBA/2J glaucoma mouse model [3,5–8]. Manganese-enhanced MRI has previously shown impaired intraretinal uptake of manganese in aged DBA/2J mice [13]. In the present study, we observed that Gd-accumulation is altered in the AC of the aged DBA/2J mouse compared to age matched C57BL/6J mice. Reduced AC signal enhancement was observed in aged DBA/2J mice in addition to lower rates of Gd-DTPA increase and lower Gd-DTPA peak intensities compared to age-matched controls. This result was in contrast to expectations, due to the reduced AH outflow in these aged animals and indicated a secondary pathology. The aged DBA/2J eyes were found to have a compromised blood-aqueous barrier, demonstrated by the posterior diffusion of Gd-DTPA from the ciliary body into the VB. Gd-DTPA is approximately 938 Da in size, so further work is required to understand the extent of blood-aqueous barrier breakdown in DBA/2J mice and in pigmentary glaucoma, for example via the systemic administration of molecular tracers of defined sizes and aqueous sampling. Ageing in DBA/2J mice was also associated with structural anomalies in ocular anatomy. Using pre-contrast MR images, AC depth was found to increase substantially with age in DBA/2J animals. This finding is in agreement with previous reports of age-associated increases in AC depth measured using ultrasound [3], slit-lamp [32] and whole-eye optical coherence tomography [33]. Indeed, this clear “bulging” of the AC observed in the MR images correlated with increased AC area, AC signal intensity and eye size in DBA/2J mice.

The use of dynamic contrast-enhanced MRI to assess flow dynamics of gadolinium-tracer from systemic circulation to the AC may also greatly advance the development of novel IOP-lowering compounds for the treatment of POAG, testing of novel conventional outflow drugs and in the study of pseudoexfoliation glaucoma which is characterized by

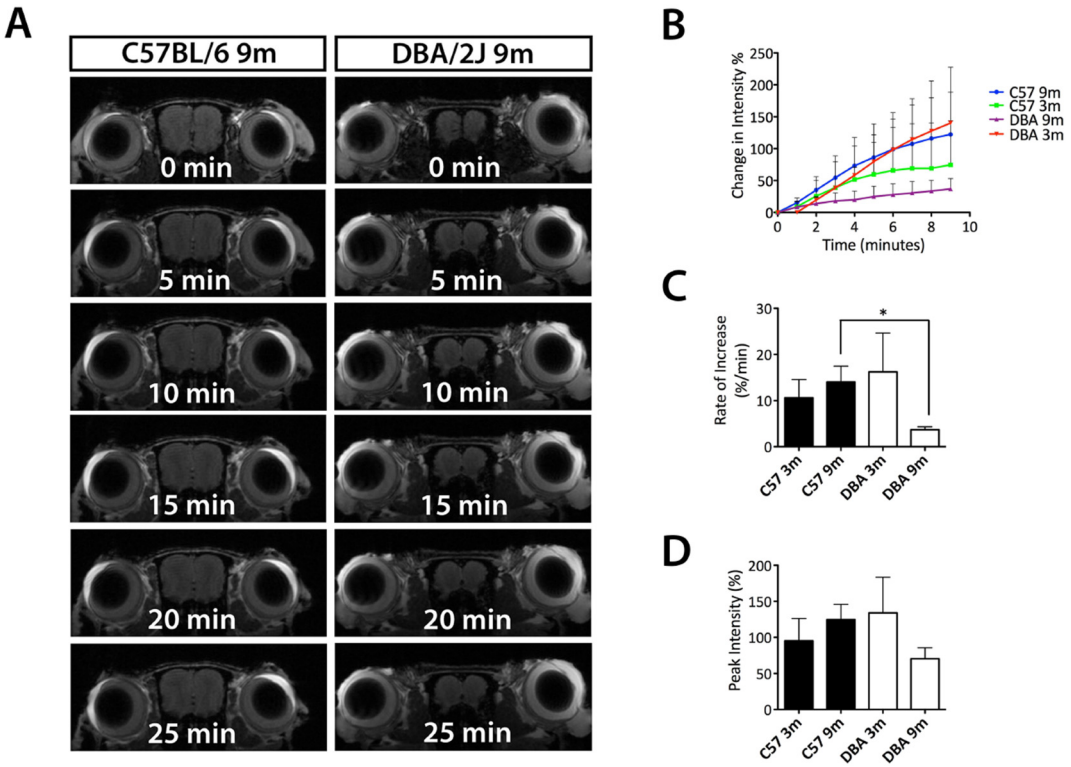

Fig. 4. Assessing aqueous humor dynamics with age in the DBA/2J model of pigmentary glaucoma using T1-weighted Gd-DTPA MRI.
A. Representative serial T1-weighted MR images of Gd-DTPA enhancement in C57BL/6 and DBA/2J mouse eyes at 9 months of age. B. Percentage change in intensity of AC in the first 10 min post-Gd-DTPA injection. Decreased levels of Gd-DTPA signal enhancement in the AC were observed in 9 month-old DBA/2J mice compared to 3 month-old DBA/2J mice and C57BL/6 mice at all ages. C. The rate of Gd-DTPA signal increase was lowest in 9 month-old DBA/2J mice compared to 3 month-old DBA/2J mice and C57BL/6 mice at all ages. D. Peak Gd-DTPA signal enhancement in the AC was lowest in 9 month-old DBA/2J mice.

extracellular deposits in the conventional outflow pathway. The dynamic aqueous humor flow changes observed in this study in both C57BL/6J and DBA/2J mice may provide important information to determine the effectiveness of long-term surgical treatments in eventual clinical studies. While the DBA/2J mice are a useful tool for glaucoma research, it must be recognized that there are shortcomings with the model and they do not recapitulate every feature of the human disease. Recently, the use of glaucoma drainage devices for both primary and refractory glaucoma such as the Baerveldt, the Ahmed or more recently the EX-PRESS has dramatically increased. These surgical implants can have serious complications such as hypotony or tube obstruction that can lead to subconjunctival fibrosis and tube failure [34]. As any intervention requires surgery, Gd-MRI offers a method to directly monitor an implant's effect on aqueous humor dynamics allowing diagnosis of tube obstruction or tube damage prior to any further surgical intervention. In addition, Gd-enhanced MRI may be used to track dynamic changes in glaucomatous eyes and provide a better understanding of the mechanisms involved in systemic delivery of drugs into the AC.

Acknowledgements

Work at the Ocular Genetics Unit at the University of Dublin, Trinity College, was supported by the European Research Council ERC-2012-AdG. We thank Rustam Rakhmatullin and Christian Kerskens of Trinity College Institute of Neuroscience for technical work with the MRI scanner.

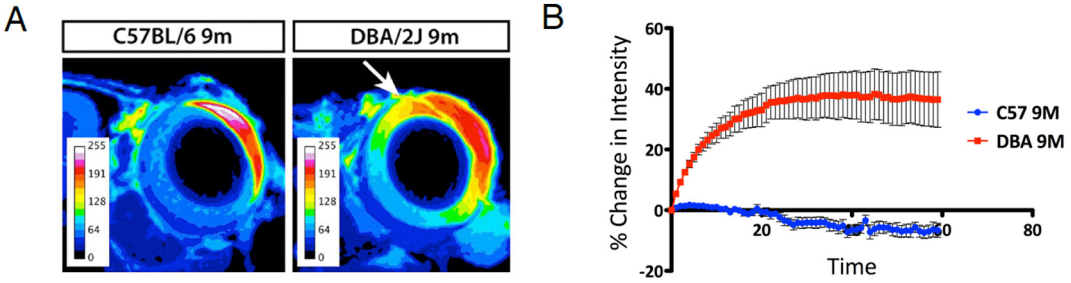

Fig. 5. Leakage of Gd-DTPA into the anterior segment of the vitreous body in DBA/2J mice.
A. Pseudocolored T1-weighted Gd-DTPA-enhanced MR images of single eyes from 9 month-old C57BL/6 and DBA/2J mice showing leakage of Gd-DTPA into the vitreous body of DBA/2J eyes (white arrow). B. Percentage change in intensity of Gd-DTPA in a region of interest located in the vitreous body close to the anterior chamber. Increased Gd-DTPA enhancement in the vitreous body of 9 month-old DBA/2J mice indicates reduced AC penetration and leakage back into the vitreous body.

References

[1] Niyadurupola N, Broadway DC. Pigment dispersion syndrome and pigmentary glaucoma - a major review. Clin Experiment Ophthalmol 2008;36:868–82.
[2] Siddiqui Y, Ten Hulzen RD, Cameron JD, Hodge DO, Johnson DH. What is the risk of developing pigmentary glaucoma from pigment dispersion syndrome? Am J Ophthalmol 2003;135:794–9.
[3] John SW, et al. Essential iris atrophy, pigment dispersion, and glaucoma in DBA/2J mice [published erratum appears in Invest Ophthalmol Vis Sci 1998 Aug;39(9):1641]. Invest Ophthalmol Vis Sci 1998;39:951–62.
[4] Zhou X, et al. Involvement of inflammation, degradation, and apoptosis in a mouse model of glaucoma. J Biol Chem 2005;280:31240–8.
[5] Saleh M, Nagaraju M, Porciatti V. Longitudinal evaluation of retinal ganglion cell function and IOP in the DBA/2J mouse model of glaucoma. Invest Ophthalmol Vis Sci 2007;48:4564–72.
[6] Inman DM, Sappington RM, Horner PJ, Calkins DJ. Quantitative correlation of optic nerve pathology with ocular pressure and corneal thickness in the DBA/2 mouse model of glaucoma. Invest Ophthalmol Vis Sci 2006;47:986–96.
[7] Jakobs TC, Libby RT, Ben Y, John SWM, Masland RH. Retinal ganglion cell degeneration is topological but not cell type specific in DBA/2J mice. J Cell Biol 2005;171:313–25.
[8] Schuettauf F, Quinto K, Naskar R, Zurakowski D. Effects of anti-glaucoma medications on ganglion cell survival: the DBA/2J mouse model. Vision Res 2002;42:2333–7.
[9] Goel M, Picciani RG, Lee RK, Bhattacharya SK. Aqueous humor dynamics: a review. Open Ophthalmol J 2010;4:52–9.
[10] Chang B, et al. Interacting loci cause severe iris atrophy and glaucoma in DBA/2J mice. Nat Genet 1999;21:405–9.
[11] Anderson MG, et al. Mutations in genes encoding melanosomal proteins cause pigmentary glaucoma in DBA/2J mice. Nat Genet 2002;30:81–5.
[12] Tkatchenko TV, Shen Y, Tkatchenko AV. Analysis of postnatal eye development in the mouse with high-resolution small animal magnetic resonance imaging. Investig Ophthalmol Vis Sci 2010;51:21–7.
[13] Calkins DJ, Horner PJ, Roberts R, Gradianu M, Berkowitz BA. Manganese-enhanced MRI of the DBA/2J mouse model of hereditary glaucoma. Investig Ophthalmol Vis Sci 2008;49:5083–8.
[14] Singh KD, Logan NS, Gilmartin B. Three-dimensional modeling of the human eye based on magnetic resonance imaging. Investig Ophthalmol Vis Sci 2006;47:2272–9.
[15] Lavery WJ, Muir ER, Kiel JW, Duong TQ. Magnetic resonance imaging indicates decreased choroidal and retinal blood flow in the DBA/2J mouse model of glaucoma. Investig Ophthalmol Vis Sci 2012;53:560–4.
[16] Berkowitz BA, et al. Dynamic contrast-enhanced MRI measurements of passive permeability through blood retinal barrier in diabetic rats. Invest Ophthalmol Vis Sci 2004;45:2391–8.
[17] Ho LC, et al. In vivo assessment of aqueous humor dynamics upon chronic ocular hypertension and hypotensive drug treatment using gadolinium-enhanced MRI. Investig Ophthalmol Vis Sci 2014;55:3747–57.
[18] Bert RJ, et al. Demonstration, of an anterior diflusional pathway for solutes in the normal human eye with high spatial resolution contrast-enhanced dynamic MR imaging. Investig Ophthalmol Vis Sci 2006;47:5153–62.
[19] Chan KC, Fu Q ling, Guo H, So K fai, Wu EX. GD-DTPA enhanced MRI of ocular transport in a rat model of chronic glaucoma. Exp Eye Res 2008;87:334–41.
[20] Cheng HM, Kwong KK, Xiong J, Chang C. GdDTPA-enhanced magnetic resonance imaging of the aqueous flow in the rabbit eye. Magn Reson Med 1991 Jan;17(1):237–43.
[21] Li L, Yuan Y, Chen L, Li M, Ji P, Gong J, et al. Gadolinium-enhanced 7.0 T magnetic resonance imaging assessment of the aqueous inflow in rat eyes in vivo. Exp Eye Res 2017 Sep;162:18–26.
[22] Tsiapa I, Tsilimbaris MK, Papadaki E, Bouziotis P, Pallikaris IG, Karantanas AH, et al. High resolution MR eye protocol optimization: comparison between 3D-CISS, 3D-PSIF and 3D-VIBE sequences. Phys Med 2015 Nov;31(7):774–80.
[23] Weinreb RN, Toris CB, Gabelt BT, Lindsey JD, Kaufman PL. Effects of prostaglandins on the aqueous humor outflow pathways. Surv Ophthalmol 2002;47:S53–64.
[24] Bahler CK, Howell KG, Hann CR, Fautsch MP, Johnson DH. Prostaglandins increase trabecular meshwork outflow facility in cultured human anterior segments. Am J Ophthalmol 2008;145:114–9.
[25] Kolodny NH, Freddo TF, Lawrence BA, Suarez C, Bartels SP. Contrast-enhanced magnetic resonance imaging confirmation of an anterior protein pathway in normal rabbit eyes. Investig Ophthalmol Vis Sci 1996;37:1602–7.
[26] Freddo TF, Neville N, Gong H. Pilocarpine-induced flare is physiological rather than pathological. Exp Eye Res 2013;107:37–43.
[27] Zhou LX, Liu JHK. Circadian variation of mouse aqueous humor protein. Mol Vis 2006;12:639–43.
[28] Bahler CK, Howell KG, Hann CR, Fautsch MP, Johnson DH. Prostaglandins increase trabecular meshwork outflow facility in cultured human anterior segments. Am J Ophthalmol 2008 Jan;145(1):114–9.
[29] Wan Z, Woodward DF, Cornell CL, Fliri HG, Martos JL, Pettit SN, et al. Bimatoprost, prostamide activity, and conventional drainage. Invest Ophthalmol Vis Sci 2007 Sep;48(9):4107–15.
[30] Lee PY, Podos SM, Severin C. Effect of prostaglandin F2 alpha on aqueous humor dynamics of rabbit, cat, and monkey. Invest Ophthalmol Vis Sci 1984 Sep;25(9):1087–93.
[31] Brubaker RF, Schoff EO, Nau CB, Carpenter SP, Chen K, Vandenburgh AM. Effects of AGN 192024, a new ocular hypotensive agent, on aqueous dynamics. Am J Ophthalmol 2001 Jan;131(1):19–24.
[32] Libby RT, et al. Inherited glaucoma in DBA/2J mice: pertinent disease features for studying the neurodegeneration. Vis Neurosci 2005;22:637–48.
[33] Chou T-H, et al. Postnatal elongation of eye size in DBA/2J mice compared with C57BL/6J mice: in vivo analysis with whole-eye OCT. Invest Ophthalmol Vis Sci 2011;52:3604–12.
[34] Giovingo M. Complications of glaucoma drainage device surgery: a review. Semin Ophthalmol 2014;29:397–402.